Detection and Quantification of Endogenous Cyclic DNA Adducts Derived from *trans*-4-Hydroxy-2-nonenal in Human Brain Tissue by Isotope Dilution Capillary Liquid Chromatography Nanoelectrospray Tandem Mass Spectrometry

Xinli Liu,[†] Mark A. Lovell,[†,‡] and Bert C. Lynn*[,†,‡]

Department of Chemistry, University of Kentucky, Lexington, Kentucky 40506-0055, and Sanders-Brown Center on Aging, University of Kentucky, Lexington, Kentucky 40536-0230

Received October 19, 2005

A sensitive and selective capillary liquid chromatography nanoelectrospray isotope dilution mass spectrometric method was developed to identify and quantify the endogenous cyclic DNA adducts derived from *trans*-4-hydroxy-2-nonenal with 2′-deoxyguanosine (HNE-dG) in human brain tissues. Authentic and ^{13}C and ^{15}N stable isotope-labeled HNE-dG were synthesized to serve as standards. The in vitro HNE-modified calf-thymus DNA as well as the DNA samples isolated from human brain tissues of normal and Alzheimer's disease subjects were enzymatically digested to nucleosides in vitro with the presence of internal standard (HNE-dG-$^{13}C_{10}$, $^{15}N_5$). The enzymatic digests were cleaned up by solid phase extraction. Only 1−2 μg of DNA digests was loaded on a laboratory-constructed reversed phase capillary chromatography column, and the HNE-dG adducts were separated from intact nucleosides and quantified by a high capacity ion trap mass spectrometer in the MS/MS mode. This method was able to quantify an adduct level of approximately 40 lesions/10^9 normal DNA nucleosides. The detected level of HNE-dG adducts in hippocampus/parahippocampal gyrus and inferior parietal regions of postmortem brains from AD subjects were 556 ± 379 and 238 ± 72 adducts per 10^9 normal nucleosides, respectively. These results were consistent with the ^{32}P postlabeling results, which detected 400−600 adducts per 10^9 normal nucleotides in the hippocampus.

Introduction

A growing body of evidence suggests that oxidative stress is a major upstream component in the signaling cascade involved in many cellular functions, such as cell proliferation, apoptosis, and inflammatory responses. Many of the effects of cellular dysfunction in oxidative stress are mediated by-products generated from the oxidation of polyunsaturated fatty acids (PUFAs),[1] which are basic biological membrane components (*1*). Increasing levels of lipid peroxidation products were detected in tissues from subjects with chronic diseases, such as asthma, Alzheimer's disease (AD), rheumatoid arthritis, burn injury, diabetes, multiple sclerosis, Parkinson's disease, stroke, and aging (*2*). *trans*-4-Hydroxy-2-nonenal (HNE) represents a major α,β-unsaturated aldehyde product with toxic potential in lipid peroxidation processes (*3*, *4*). Since its discovery by Esterbauer and coworkers, HNE has been extensively studied as a marker of lipid peroxidation and recognized as the "second toxic messengers of free radicals" (*5*), "one of the most physiologically active lipid peroxides" (*6*), and "one of the major generators of oxidative stress" (*7*). HNE was reported as the major product from oxidized ω-6 PUFAs (*8*). Endogenous formation of HNE was detected in various tissues isolated from rodents and humans with estimated levels varying from 0.3 to 8 nmol/mg, depending on the tissues and pathological conditions (*3*).

HNE has an enal functionality (a bis-electrophile) and can react with deoxyguanosine through an initial Michael addition of the exocyclic amino group followed by ring closure of N-1 onto the aldehyde group to generate the HNE-derived cyclic 1,N^2-propanodeoxyguanosine adducts (HNE-dG adducts, Scheme 1). The reaction of deoxyguanosine with HNE gives three new stereogenic centers. The relative stereochemistry of the C8-hydroxy group and the C6-hydroxyalkyl side chain is trans (*9*, *10*). Four diastereomeric adducts (6*R*,8*S*,11*R*), (6*S*,8*R*,11*S*), (6*R*,8*S*,11*S*), and (6*S*,8*R*,11*R*) are possible (*11*). The C-11 sterochemistry is derived from HNE, which is presumably produced in a racemic form from lipid peroxidation. Thus, two diastereomers (6*R*,8*S*,11*R*)-HNE-dG and (6*S*,8*R*,11*R*)-HNE-dG adducts are derived from the *R* enantiomer (4*R*-HNE), and another two diastereomers (6*S*,8*R*,11*S*)-HNE-dG and (6*R*,8*S*,-11*S*)-HNE-dG adducts are derived from the *S*-enantiomer (4*S*-HNE).

Multiple studies have demonstrated that the brain in AD contains extensive oxidative damage, since neurons are postmitotic cells that can gradually accumulate oxidative damage over time (*12*). The latest reports indicate that lipid peroxidation occurs early in the pathogenesis of AD and is not a late effect of the neurodegenerative process (*13*). Using mass spectrometric detection, a statistically significant elevation of free HNE has been detected in an AD disease progression-related manner in brain tissue (*14*).

* To whom correspondence should be addressed. Tel: 859-257-2300 ext. 287. Fax: 859-257-2489. E-mail: bclynn2@uky.edu.
[†] Department of Chemistry.
[‡] Sanders-Brown Center on Aging.

[1] Abbreviations: PUFAs, polyunsaturated fatty acids; HNE, *trans*-4-hydroxy-2-nonenal; HNE-dG, deoxyguanosine adducts of *trans*-4-hydroxy-2-nonenal; capLC-nanoESI-IDMS/MS, capillary liquid chromatography nanoelectrospray isotope dilution tandem mass spectrometry; AD, Alzheimer's disease; ctDNA, calf thymus DNA; IPL, inferior parietal lobule; HPG, hippocampus and parahippocampal gyrus.

10.1021/tx0502903 CCC: $33.50
Published on Web 04/11/2006

Scheme 1. Formation of the Four Stereoisomeric HNE-dG Adducts from the Reaction of 2′-Deoxyguanosine with HNE

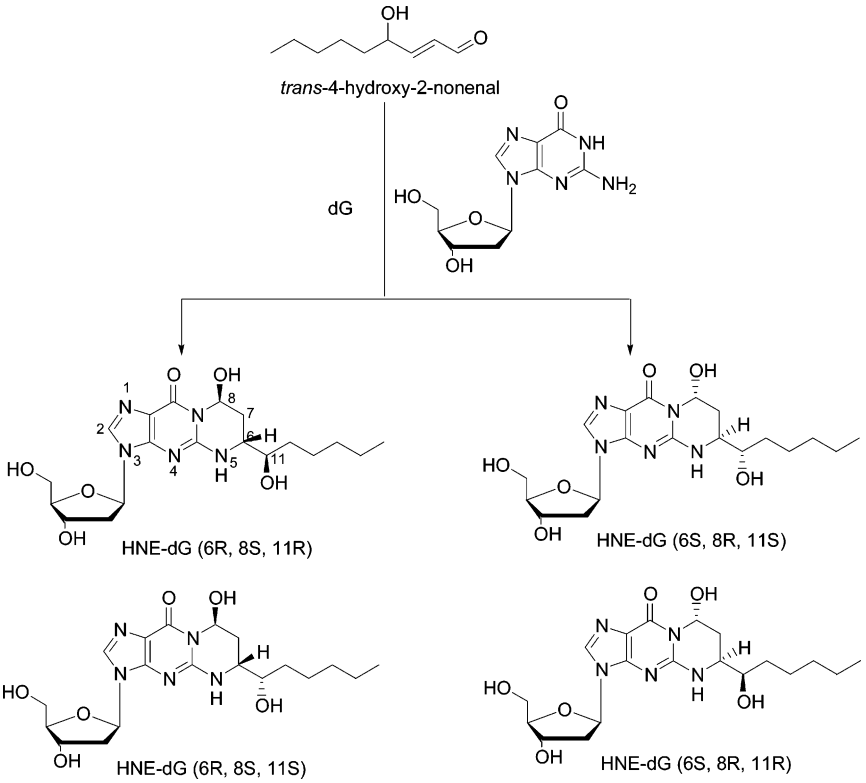

Recent reviews by Farmer and co-workers (*15*, *16*) describe the contributions of mass spectrometry in quantifying DNA adducts. The reviewers comment that a major challenge facing DNA adduct researchers is the need for enhanced sensitivity (1 adduct per 10^8 unmodified bases) from low microgram quantities of DNA. This challenge is especially critical for AD research where tissue samples from areas of high pathology such as the hippocampus are extremely limited and in high demand from many research groups. Thus, the largest amount of DNA available for AD hippocampus adduct studies would be approximately 10 μg.

To explore the possibility that HNE-DNA adducts can serve as novel and useful markers for the occurrence and/or the extent of oxidative stress in AD, we describe here a sensitive and specific capillary liquid chromatography nanoelectrospray isotope dilution tandem mass spectrometry (capLC-nanoESI-IDMS/MS) method to quantify endogenous HNE-dG levels in brain tissue. This is the first report of detecting and quantifying HNE-dG adducts in vivo using a method other than a highly sensitive ^{32}P-postlabling method. Fu and co-workers described a ^{32}P-postlabeling/HPLC method for quantification of this adduct at nucleotide levels (1,N^2-propanodeoxyguanosine 3′-monophosphate or HNE-dGp) with a detection limit between 1.2 adducts/10^8 nucleotides and 5 adducts/10^9 nucleotides for pure standard (*17*). Using a similar method, Chung et al. reported that HNE-dGp adducts are present as background DNA lesions in rodent and human tissues with estimated amounts in the range of 3−9 nmol adducts/mol guanine (*18*, *19*). Eder et al. also developed a ^{32}P-postlabeling method with a sensitivity of approximately 21 adducts/10^9 nucleotides in the presence of DNA matrix (*20*). The capLC-nanoESI-IDMS/MS method reported here was found to be sensitive and accurate enough to detect HNE-dG in the femtogram range using ∼1−2 μg of DNA. Application of the developed method to the analysis of brain tissues isolated from AD and age matched control subjects revealed that endogenously generated HNE-dG adducts in hippocampus/parahippocampal gyrus regions were detected at a level of 556 ± 379 adducts per 10^9 normal nucleosides in AD relative to 464 ± 316 adducts per 10^9 normal nucleosides in DNA from control subjects.

Experimental Procedures

Caution: *HNE is highly cytotoxic and mutagenic and should be handled using gloves in a well-ventilated hood.*

Chemicals and Materials. Fumaraldehyde bis(dimethyl acetal), pentylmagnesium bromide, and Amberlyst-15 ion-exchange resin were purchased from Aldrich (Milwaukee, WI). 2′-Deoxyguanosine, deoxyribonuclease I (from bovine pancrease), phosphodiesterase I (from *Crotalus adamanteus* venom), phosphodiesterase II (from bovine spleen), and alkaline phosphatase were obtained from Sigma (St. Louis, MO). Calf thymus DNA (ctDNA) was purchased from Worthington Biochemical Co. (Lakewood, NJ). 2′-Deoxyguanosine-$^{13}C_{10}$,$^{15}N_5$-5′-triphosphate sodium salt (dGPT-$^{13}C_{10}$,$^{15}N_5$, U-$^{13}C_{10}$, 98%; U-$^{15}N_5$, 98%) was obtained from Isotec (Miamisburg, OH). HPLC grade water, acetonitrile, and formic acid were purchased from Fisher Scientific (Fair Lawn, NJ). An Oasis HLB 30 mg solid phase extraction (SPE) cartridge was obtained from Waters (Milford, MA). Fused silica capillary tubing (100 μm i.d. × 358 μm o.d.) (Polymicro Tech., Phoenix, AZ) was used in column fabrication. PolymerX 3 μm stationary phase packing material was obtained from Phenomenex (Torrance, CA).

Synthesis of Racemic HNE. HNE was synthesized by utilizing an effective and selective mono-hydrolysis of the commercially available *trans*-fumaraldehyde bis(dimethyl acetal) using Amberlyst-15 catalyst to generate fumaraldehyde monodimethyl acetal (*21*), which upon reaction with Grignard reagent $C_5H_{11}MgBr$ produced HNE-dimethyl acetal (*22*). HNE was obtained from hydrolysis product of HNE-dimethyl acetal with Amberlyst-15 catalyst. The structure and purity of HNE were established by NMR and GC-MS.

Synthesis of Adduct Standards. Aliquots of HNE were reacted with 10 equiv of each of the four deoxynucleosides, 2′-deoxyguanosine (dG), 2′-deoxyadenosine (dA), 2′-deoxycytidine (dC), and thymidine (dT), in 1 mL of phosphate buffer (25 mM, pH 7.4) at

37 °C for 7 days. Stable isotope-labeled analogues of HNE-dGTP-$^{13}C_{10}$,$^{15}N_5$ were prepared from incubation of HNE (~10 equiv) with 2′-deoxyguanosine-$^{13}C_{10}$,$^{15}N_5$-5′-triphosphate (dGTP-$^{13}C_{10}$,$^{15}N_5$) in phosphate buffer (25 mM, pH 7.5) at 37 °C for 7 days. Unreacted HNE was extracted with methylene chloride. HNE-dGTP-$^{13}C_{10}$,$^{15}N_5$ was dissolved in 1 mL of 4 mM Tris-HCl buffer (pH 8.0) and incubated with alkaline phosphatase (4 units/mg sample) at 37 °C for 24 h to generate HNE-dG-$^{13}C_{10}$,$^{15}N_5$. The enzyme was removed using a Millipore centrifugal filter with a molecular mass cutoff of 5 kDa at 6000*g* for 1 h. Subsequently, the crude isotope-labeled and unlabeled adducts, respectively, were dried by vacuum centrifugation and redissolved in water for semipreparative HPLC purification using the LC-UV-system 1 equipped with a Thermo Separation SpectraSYSTEM P4000 pump and a UV6000LP detector (Themo Separation Products, San Jose, CA). Crude products were separated on a reversed phase Phenomenex Luna 5 μm 250 mm × 4.60 mm C18 column (Phenomenex) with an isocratic condition (water:acetonitrile 75:25, v/v, detection at 260 nm) at flow rate of 1 mL/min over 30 min. Adduct fractions were collected and their composition and purity verified by full scan mass spectrometry (*m*/*z* 100−600).

HNE Modification of DNA in Vitro. HNE-modified ctDNA was generated by incubating ctDNA (250 μg, ~0.75 μmol of nucleotides) with a 10-fold excess of HNE (7.5 μmol, ~33 μL) in 5 mM Tris/10 mM $MgCl_2$, pH 8.5, buffer at 37 °C for 7 days. Excess HNE was removed by methylene chloride extraction, and the DNA was recovered by chilled ethanol precipitation. Control ctDNA and HNE-modified ctDNA samples were spiked with the isotope-labeled internal standard HNE-dG-$^{13}C_{10}$,$^{15}N_5$ and hydrolyzed enzymatically to nucleosides with deoxyribonuclease I (DNase I from bovine pancreas, 200 U/mg DNA), *C. adamanteus* venom phosphodiesterase I (5′ exonuclease, 0.3 U/mg DNA), bovine spleen phosphodiesterase II (3′-exonuclease, 0.01 U/mg DNA), and alkaline phosphatase (10 U/mg DNA) in the presence of 4 mM Tris HCl (pH 8.0) containing 10 mM $MgCl_2$ at 37 °C for 24 h. Enzyme digests were then subjected to SPE using the Oasis HLB cartridge. The SPE cartridge was washed with a mixture of water and methanol (95/5, v/v) to remove the major polar normal nucleosides. HNE-dG adducts were recovered by eluting with pure methanol, dried, and reconstituted in mobile phase for LC-MS analysis.

LC-MS Analysis. Quantification of HNE-dG adducts was performed on a capillary LC (Ultimate, LC Packings, Sunnyvale, CA) coupled to a Bruker HCT high capacity ion trap mass spectrometer (Bruker Daltonics, Billerica, MA) through a nano-electrospray interface. The mass analysis was conducted in the tandem mode. The combined experiment was referred to as capLC-nanoESI-IDMS/MS. The chromatographic column consisted of a 100 μm i.d. bare fused silica capillary column packed with reversed phase Phenomenex PolymerX particles (3 μm polystyrene divinylbezene polymer, 16 cm long) according to previously described procedures (*23*, *24*). The separation was achieved using isocratic conditions (75% mobile phase A consisted of 0.1% aqueous formic acid and 25% mobile phase B of 0.1% formic acid in acetonitrile). All capillary analyses used 5 μL injection volumes. The pump output (150 μL/min) was split before the injection port to a flow rate of 500 nL/min. The spray voltage was set between −1400 and −1600 V to achieve a stable current. Heated nitrogen drying gas (3.0 L/min, 200 °C) was introduced in the spray chamber to aid in desolvation. The mass spectrometer was configured for two alternating scan segments. The first segment was a scan of product ions ($[M - 116 + H]^+$: *m*/*z* 308) produced from protonated HNE-dG ($[M + H]^+$: *m*/*z* 424) isolated in a window 3 *m*/*z* wide. The second segment was a scan of product ions ($[M - 121 + H]^+$: *m*/*z* 318) produced from protonated HNE-dG-$^{13}C_{10}$,$^{15}N_5$ ($[M + H]^+$: *m*/*z* 439) isolated in a window 3 *m*/*z* wide.

A calibration curve was plotted for the integrated peak area ratio of nonlabeled HNE-dG vs HNE-dG-$^{13}C_{10}$,$^{15}N_5$ (peak area of the ion *m*/*z* 308 divided by peak area of the *m*/*z* 318) against the standard HNE-dG at an amount range of 0.1−150 pg (0.1, 2, 4, 8, 10, 15, 20, 25, 50, and 150 pg) on column. Blank injections both with and without internal standard and with and without ctDNA hydrolysate were also analyzed to verify that there was no cross-contamination in the ion detection windows for HNE-dG or for nonadducted nucleoside bases in native DNA.

Isolation of Human Brain DNA. Brain tissues used in this study were removed at autopsy from AD subjects and age-matched control subjects per University of Kentucky approved IRB protocols immediately frozen in liquid nitrogen, and subsequently stored at −80 °C. All AD subjects met the National Institute on Aging-Reagan Institute guidelines (*25*) for the histopathologic diagnosis of AD. Control subjects were without a history of dementia or other neurologic disorders. Neuropathologic evaluation of control brains revealed only age-associated gross and histopathologic changes. Braak staging (Braak score) was used as autopsy criterion for the diagnosis of AD (*26*).

To isolate DNA for HNE-dG adducts determinations, tissue was homogenized and nuclear DNA were isolated using a previously described procedure (*27*). Briefly, tissue specimens from the hippocampus/parahippocampal gyrus (HPG) and inferior parietal lobule (IPL) were homogenized on ice using a Teflon-coated Dounce homogenizer in MSB-Ca^{2+} buffer (0.21 M mannitol, 0.07 M sucrose, 0.05 M Tris-HCl, and 3 mM $CaCl_2$, pH 7.5). The homogenate was centrifuged at 1500*g* for 20 min. The supernatant was removed, and the pellet was resuspended in MSB-Ca^{2+} buffer and centrifuged again. The resulting pellet fraction was resuspended in digestion buffer (0.5% sodium dodecyl sulfate, 0.05 M Tris-HCl, and 0.1 M Na_2EDTA) and incubated with 400 μg/mL proteinase K in a 55 °C water bath overnight. Then, 160 μL of 5 M NaCl per 10 mL crude solution was added, followed by extraction three times with buffer-saturated phenol containing 5.5 mM 8-hydroxyquinoline and three times with chloroform/isoamyl alcohol (24:1). Precipitated DNA was obtained by adding 800 μL of 5 M NaCl per 10 mL clear suspension and an equal volume of chilled absolute ethanol. After centrifugation, the DNA pellet was washed three times with 60% alcohol and air-dried. The DNA pellet was dissolved in autoclaved water, and the concentration of DNA was determined at 260 nm ($A_{260} = 1$ at 50 μg/mL). Absorbance was also measured at 280 nm, with a mean 260/280 ratio less than 2 indicating a relatively pure DNA preparation with little or no contamination by proteins or RNA. The DNA was stored at −80 °C prior to the analysis, and the same enzymatic digestion procedure was carried out as in vitro HNE-modified ctDNA samples.

Statistical Analysis. HNE-dG adducts level are presented as means ± standard deviations. To determine if the averages of two samples were significantly different, statistical analysis using an unpaired Student's *t*-test was performed using the commercially available SigmaPlot 8.0 software (Systat Software Inc., CA). A $P < 0.05$ was considered significant.

Results and Discussion

Reactivity of HNE with Deoxyguanosine. In vitro reaction of HNE with four different nucleosides (dA/dT/dG/dC) showed that the deoxyguanosine was the most reactive nucleoside. The majority of deoxyguanosine was converted to HNE-dG adducts. In contrast, free nucleosides dA, dC, and dT remained as the major components of the above reaction mixtures. Small amounts of adducts were generated from the HNE reaction with dA but not observed from the reaction with dC and dT. Because HNE-dG was the major product from the reaction of HNE with nucleosides, we focused our attention on the identification and quantification of HNE-dG adducts in the DNA samples.

To obtain a pure HNE-dG standard, HNE and HNE-dG adducts were synthesized and crude products from HNE and dG reaction were purified by LC-UV-system 1. A typical HPLC-UV chromatogram is shown in Figure 1; each peak was collected separately and identified using LC-MS. Unreacted deoxyguanosine eluted first (*m*/*z* = 268), followed by a peak with a retention time of 3.9 min, which was identified as guanine based

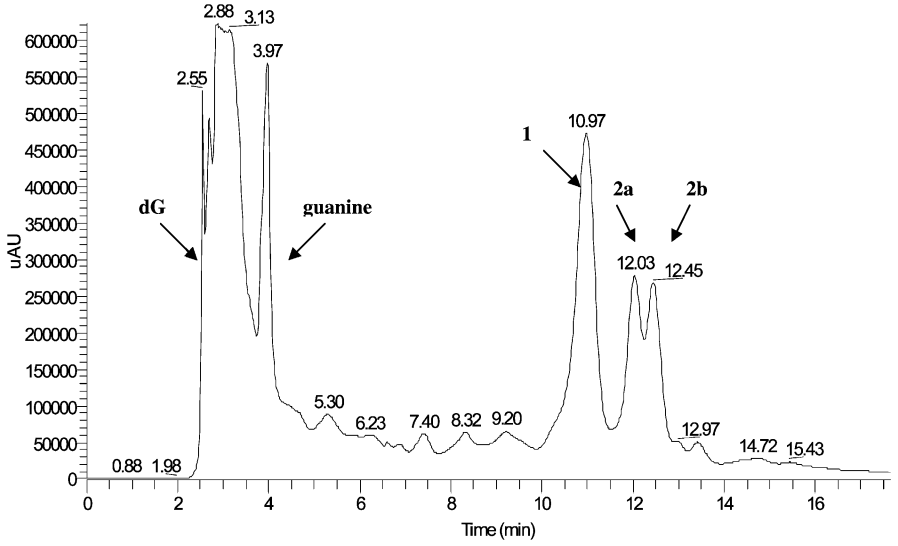

Figure 1. Chromatogram obtained by HPLC purification of reaction mixtures of HNE and deoxyguanosine. Separation was achieved on a Phenomenex Luna 5 μm 250 mm × 4.60 mm C18 column with an isocratic separation (water:acetonitrile, 75:25, v/v) at flow rate of 1 mL/min over 30 min at 260 nm. Free deoxyguanosine (T_R = 2.88) and guanine (T_R = 3.97) eluted first. Peaks 1, 2a, and 2b were HNE-dG adducts. Only peak 1 was used as an authentic standard for the calibration assay.

on mass spectral data *m*/*z* 152 ($[M + H]^+$). Three major chromatographic peaks eluting at 10.97, 12.03, and 12.45 min (labeled as 1, 2a, and 2b, respectively) represented different stereoisomers of cyclic HNE-dG adducts (*m*/*z* 423). Under similar collision-induced dissociation (CID) conditions, their mass spectra were identical. Definitive stereochemical assignment was made on the basis of reported individual chromatographic retention. According to Rizzo and co-workers, four stereochemically defined HNE-dG adducts were synthesized individually and the chromatographic behaviors of each stereoisomer as well as a mixture of the four were studied (our conditions were similar to those reported) (*28*). The first fraction of HNE-dG adducts (peak 1) obtained was a pair of diastereomers (6*R*,8*S*,11*S*) and (6*S*,8*R*,11*R*). Fraction 2a was (6*R*,8*S*,-11*R*), and fraction 2b was assigned as (6*S*,8*R*,11*S*), in which the different configurations in the side chain of the newly formed ring (11*R*/*S*) originated from racemic HNE obtained in the previous synthesis procedure. This assignment was also confirmed by a comparative investigation of the retention times of both the HNE-dGp adducts and the dephosphorylated HNE-dG adducts by Fu et al. (*17*). These authors reported a partial separation of four stereoisomers of the HNE-dGp 3′,5′-bisphosphate adduct at the nucleotide level by reversed phase HPLC. A pair of diastereomeric HNE-dGp 3′,5′-bisphosphate adducts gave one peak while another pair gave two resolved peaks. Because our goal is to quantify HNE-dG adducts in DNA derived from a limited amount of biological tissues, we were more interested in total amounts of all HNE-dG adducts rather than individual diastereomers, especially considering the low incidence of HNE-dG adducts (range from 1 in 10^6 to 10^9 normal nucleosides) *in vivo*. Only one fraction (peak 1 in the Figure 1), which was comprised of a pair of diastereomers (6*R*,8*S*,11*S*) and (6*S*,8*R*,11*R*), was used as an authentic standard in constructing the calibration curve.

In previously reported ^{32}P-postlabeling assays, quantification is to a certain extent compromised by the lack of internal standards or the fact that only homologous or structural analogues were used as internal standards, which can result in variable sample recovery and detector response (*19*, *29*). In this study, isotope dilution mass spectrometry (IDMS) was pursued due to the specificity and sensitivity of this approach. Additionally, IDMS can compensate for method variations since the isotope-labeled internal standard has essentially the same chemical and physical properties as the analyte. Because only dGTP-$^{13}C_{10}$,$^{15}N_5$ was commercially available, HNE-dGTP-$^{13}C_{10}$,$^{15}N_5$ was prepared from freshly synthesized HNE and dGTP-$^{13}C_{10}$,$^{15}N_5$. The dephosphorylated product HNE-dG-$^{13}C_{10}$,$^{15}N_5$ was obtained by enzymatic reaction of HNE-dGTP-$^{13}C_{10}$,$^{15}N_5$ with alkaline phosphatase. Similarly, only a pair of diastereomers HNE-dG-$^{13}C_{10}$,$^{15}N_5$ (6*R*,8*S*,11*S*) and (6*S*,8*R*,11*R*) were used as an internal standard in subsequent analyses. The isotopic purity and chemical composition of the purified HNE-dG-$^{13}C_{10}$,$^{15}N_5$ were determined by LC-MS full scan and LC-UV with a purity >98%. This assay also revealed that no HNE-dG was detected when 5 μL of a concentrated fraction of HNE-dG-$^{13}C_{10}$,$^{15}N_5$ internal standard was injected to LC-MS.

Reaction of HNE with ctDNA. Initially, we tested the ability of HNE to modify the ctDNA in vitro. A microbore C18 column was used to separate the HNE-modified ctDNA hydrolysates. Figure 2 shows a comparison of full scan chromatogram and mass spectra of HNE-dG adducts synthesized directly from deoxyguanosine (panel A) and HNE-dG adducts obtained from hydrolysis of HNE-modified ctDNA in vitro (panel B). The microbore C18 column (1.0 mm i.d. × 15 cm, 3 μm) was able to resolve all four diastereomers as compared to the conventional analytical column (4.60 mm i.d. × 25 cm, 5 μm) used in the purification procedure (smaller particles provide higher peak capacity and better resolution). Each isomer produced a *m*/*z* 424, protonated molecular ion, $[M + H]^+$. Interestingly, all four diastereomers were generated from HNE-treated ctDNA. One pair of diastereomers (6*R*,8*S*,11*S* and 6*S*,8*R*,11*R*) coeluted as a broad peak, which may indicate a dynamic conversion of these two diastereomers on the chromatographic column. These results clearly indicated a lack of steric preference when HNE reacts with helical DNA *in vitro*. Additionally, these observations were consistent with a mutagenic study that suggested that the *S*-enantiomer (4*S*-HNE) and *R*-enantiomer (4*R*-HNE) produce roughly equivalent point mutation frequencies (*30*). It should be pointed out that previously reported ^{32}P-postlabeling methods detected only two of the four possible diastereomeric adducts in HNE-treated ctDNA (*17*). The differences in chromatographic resolution of all adducts isomers in the ^{32}P-postlabeling method vs the present one is most likely because of the different analytes

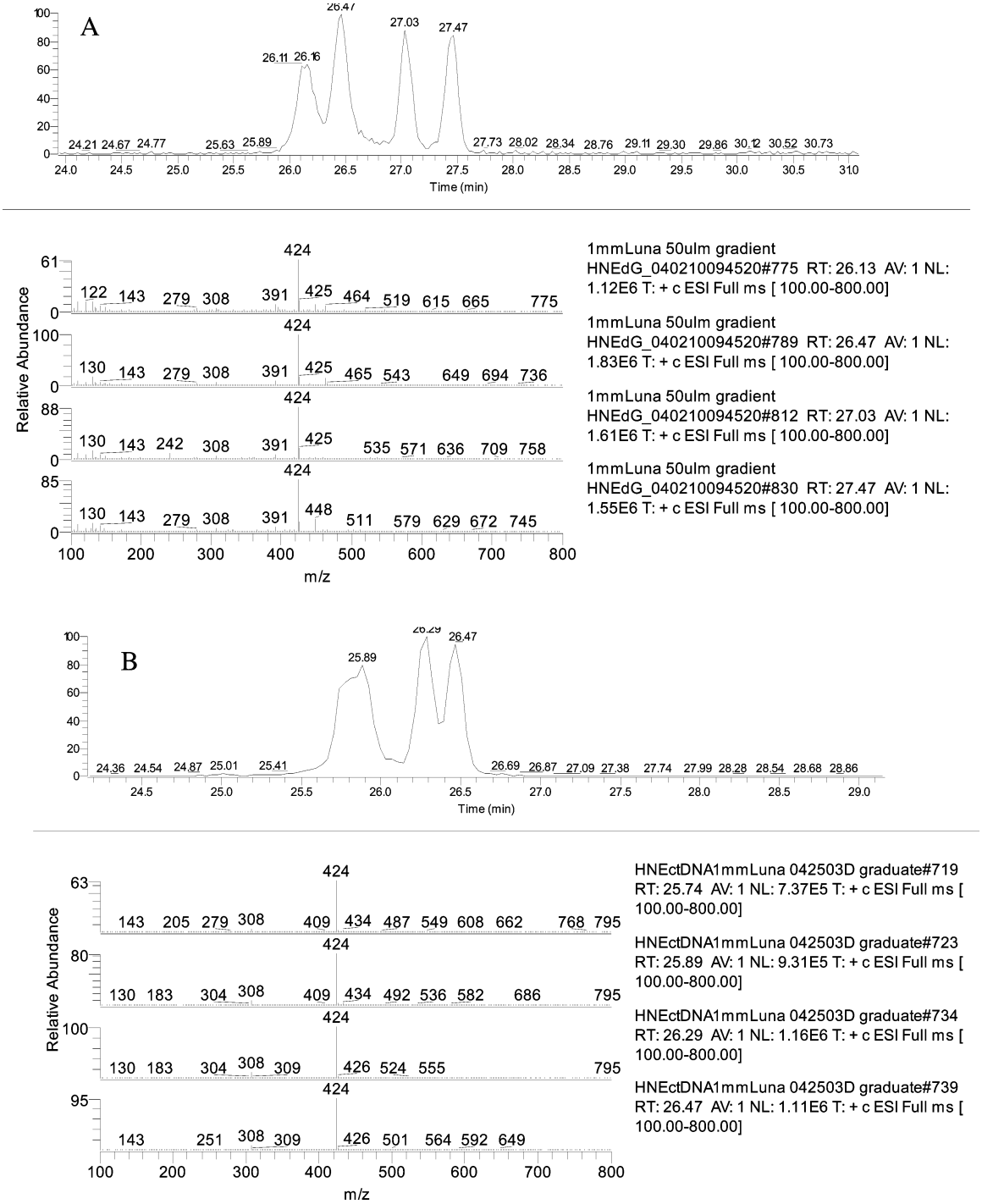

Figure 2. Comparison of full scan chromatogram and mass spectra of HNE-dG adducts synthesized directly from deoxyguanosine (A) and HNE-dG adducts obtained from the hydrolysate of HNE-modified ctDNA *in vitro* (B).

being measured (i.e., HNE-dG-bis-phosphate isomers vs HNE-dG isomers).

Quantification of HNE-dG. To improve the sensitivity of the LC-MS assay, we decreased the column inner diameter from microbore to capillary and utilized a nanoelectrospray interface that decreased sample dilution and increased detection sensitivity. Quantification of HNE-dG adducts was achieved by the capLC-nanoESI-IDMS/MS method using HNE-dG-$^{13}C_{10}$,$^{15}N_5$ as an internal standard. Figure 3 shows a typical ion chromatogram and tandem mass spectra obtained from two alternating scans of pure HNE-dG and HNE-dG-$^{13}C_{10}$,$^{15}N_5$. Chromatographically, the native and isotopically labeled compounds exactly coeluted (no isotope effect on elution behavior). Full scan spectra showed *m*/*z* 439 for HNE-dG-$^{13}C_{10}$,$^{15}N_5$, which was shifted 15 u as compared to the molecular ion from HNE-dG at *m*/*z* 424. Tandem spectra revealed an abundant product ion (*m*/*z* 318) observed from HNE-dG-$^{13}C_{10}$,$^{15}N_5$ that was consistent with loss of the deoxyribose moiety (121 u) from the precursor ion. Unlabeled HNE-dG behaved similarly by losing the unlabeled deoxyribose moiety (116 u) to produce a product ion *m*/*z* 308.

A decrease from 1 mm (microbore column) to 100 μm (capillary column) resulted in a flow rate decrease from 50 μL/min to 500 nL/min. This led to an approximately 10-fold increase of the peak concentration of the analyte delivered to the mass spectrometer using the same sample injection volume (*31*), thus enhancing sensitivity (*24*). Using an authentic HNE-dG standard, an instrument limit of detection (LOD, signal-to-

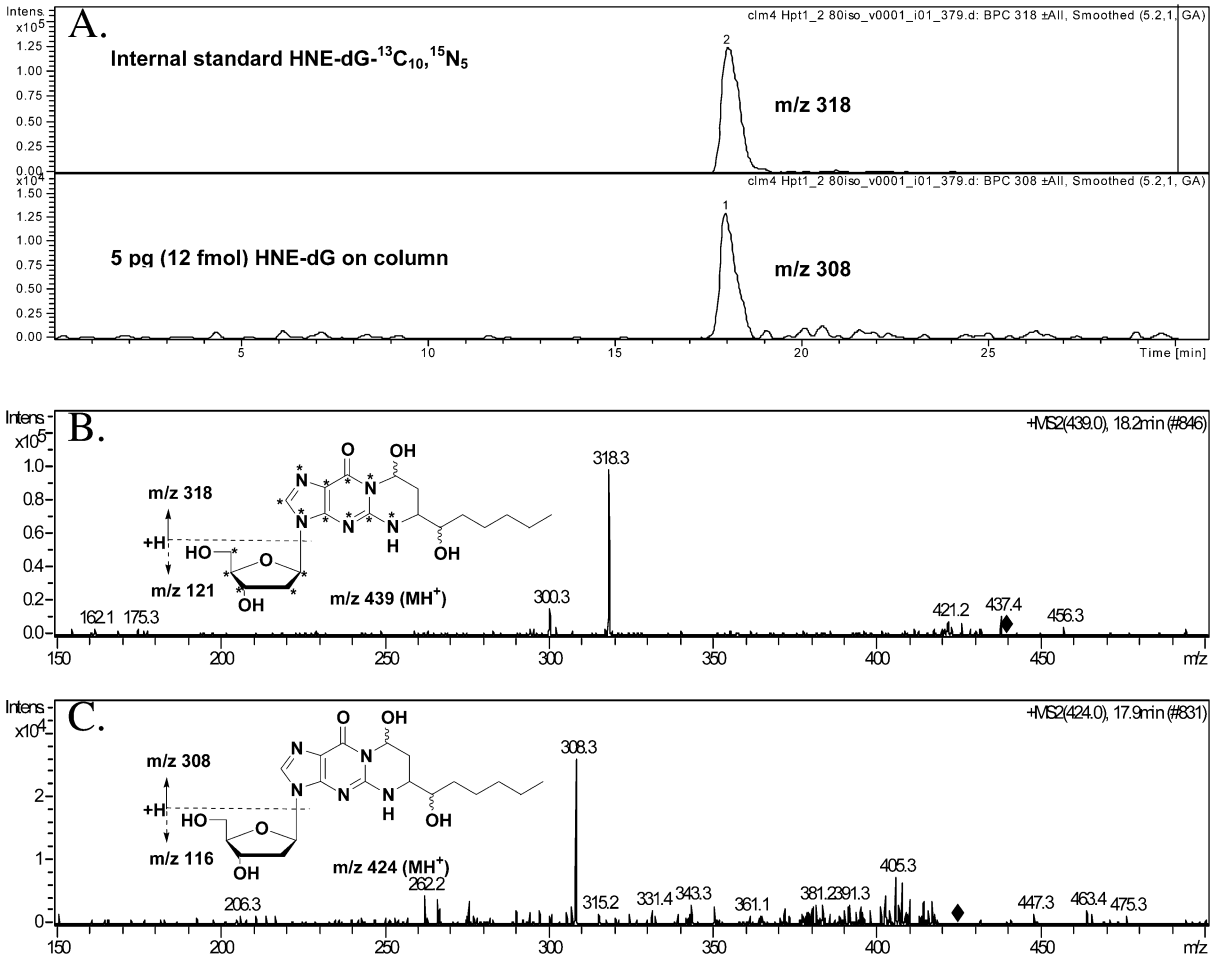

Figure 3. (A) Reconstructed ion chromatograms of *m*/*z* 318 (HNE-dG-$^{13}C_{10}$-$^{15}N_5$) and *m*/*z* 308 (HNE-dG) recorded during the capLC/nanoESI-IDMS/MS analysis. Solvents, water and acetonitrile (75/25, v/v, with 1% formic acid); flow rate, 500 nL/min. (B) Tandem mass spectrum of HNE-dG-$^{13}C_{10}$-$^{15}N_5$ (*m*/*z* 439 → *m*/*z* 318). (C) Tandem mass spectrum of HNE-dG (*m*/*z* 424 → *m*/*z* 308). Inserts show structures and fragmentation pathways of HNE-dG-$^{13}C_{10}$-$^{15}N_5$ and HNE-dG. The stars indicate the labeled atoms in HNE-dG-$^{13}C_{10}$-$^{15}N_5$.

noise ratio of ∼3) was determined to be 10 fg (24 amol) on column. The instrument limit of quantification (LOQ, signal-to-noise ratio of ∼10) was 100 fg (236 amol) on column (Figure 4). The method LOQ in the presence of complex ctDNA digests was determined by spiking standard HNE-dG into untreated ctDNA hydrolysate. A signal-to-noise of ∼10 was obtained when 500 fg of standard HNE-dG was spiked into 10 μg of DNA and the entire sample (equivalent to 10 μg of DNA) was loaded on column. This 500 fg spike was equivalent to 1.2 fmol of HNE-dG in 32 nmol of DNA (10 μg) and corresponded to a level of 40 adducts/10^9 normal nucleosides. This method achieved comparable sensitivity to the ^{32}P-postlabeling method (21 adducts/10^9 nucleotides) reported by Eder et al. (*20*) for detecting HNE-dG adducts in the presence of DNA matrix. The described capLC-nanoESI-IDMS/MS provides improved features over existing ^{32}P-postlabeling methods such as avoidance of handling radioisotopes; however, capillary HPLC has several potential drawbacks such as decreased column loading capacity and that fact that capillary columns are more prone to column plugging as compared to conventional HPLC columns.

Quantitative calibration of the assay was performed by the addition of a fixed amount of HNE-dG-$^{13}C_{10}$,$^{15}N_5$ (50 pg/μL, 250 pg on column) internal standard to various quantities of authentic standard solution of HNE-dG ranging from 0.1 to 150 pg on column (corresponding to 236 amol to 355 fmol). The characteristic *m*/*z* 318 product ion of the HNE-dG-$^{13}C_{10}$,$^{15}N_5$ and corresponding product ion *m*/*z* 308 ions of the HNE-dG were recorded simultaneously. Integrated peak area ratios (peak area of the ion *m*/*z* 308 divided by peak area of the *m*/*z* 318) were plotted against the amount of authentic HNE-dG injected on column (0.1−150 pg). A linear response to the amount HNE-dG on column was observed ($y = 0.0153x + 0.0005$) using the method of least squares with a resulting correlation coefficient R^2 of 0.9986. The precision of the method was determined by the triplicate analyses of adducts at all concentrations utilized for the construction of calibrations. A percent relative standard deviation (RSD) ranging from 1 to 8% was obtained across the standard curve range. The assay was checked for interday precision, accuracy, and linearity by acquiring standard curve data along with spiked quality control samples (with or without DNA matrix) on different days. Data from all quality control samples were within ±8% RSD.

The method was also applied to the analysis of control ctDNA and HNE-treated ctDNA using the HNE-dG-$^{13}C_{10}$,$^{15}N_5$ internal standard. A 5 μL aliquot of sample was loaded onto the capillary column, which corresponded to 50 ng of DNA digest and 250 pg of internal standard injected on column. An abundant *m*/*z* 308 peak was observed in the tandem spectrum, which corresponded to 664 pg (1.57 pmol) of HNE-dG adduct in the 50 ng HNE-treated ctDNA digest, equivalent to an adduct level of 9984 adducts/10^6 normal nucleosides. On the basis of the equation "1 nmol of a lesion/mg DNA = 308 lesions/10^6 DNA bases" (*32*), this result indicated that when excess HNE reacted with ctDNA, roughly one dG in every 25 dG (assume a quarter of dG in all nucleosides) would react with HNE to generate the cyclic HNE-dG adduct.

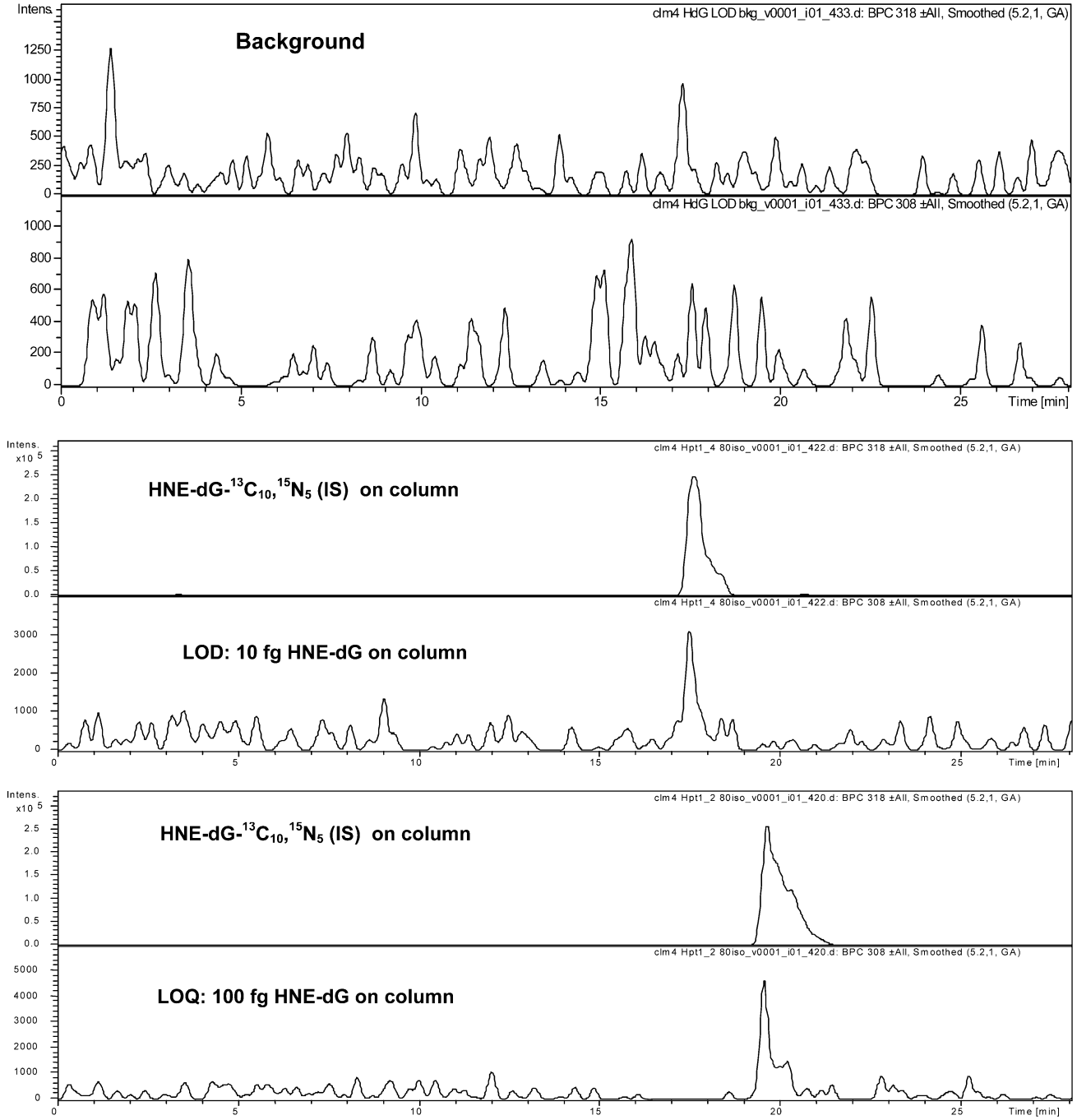

Figure 4. LOD and LOQ of HNE-dG on a 100 μm i.d. × 15 cm RP-PolymerX capillary column.

HNE-dG Adducts in Human Brain Tissues. Lovell et al. demonstrated that free HNE was significantly elevated in the amygdala of AD subjects (0.486 ± 0.096 nmol/mg protein) as compared to age-matched controls (0.193 ± 0.062 nmol/mg protein) and in HPG in AD (0.543 ± 0.123 nmol/mg protein) as compared with controls (0.256 ± 0.056 nmol/mg protein) using 1,3-cyclohexanedione derivatization, HPLC, and a fluorescence detection method (*33*). Additionally, a significant increase in free HNE (2.5-fold) in AD ventricular fluid as compared with controls was also observed; however, no significant differences in protein-bound HNE between AD and control subjects were observed (*34*). In the present study, we evaluated HNE-modified DNA adduct levels in the HPG and IPL (regions showing histopathological alterations in AD) from postmortem brain tissue samples isolated from AD and age-matched control subjects.

A total of 13 DNA samples from HPG [eight AD (four females and four males) and five age-matched controls (two females and three males)] as well as eight DNA samples from IPL [four AD (two males and two females) and four controls (two females and two males)] were obtained with high purity. Subject demographic data, postmortem interval, and Braak scores (AD pathology) are presented in Table 1. Unpaired Student's *t*-test comparisons of mean age and postmortem interval times indicated no statistically significant differences between the samples from AD and the control subjects. Analyses were performed blinded. The code was broken after the entire study was completed.

Brain nuclear DNA samples (10 μg, 32 nmol) were hydrolyzed in the presence of the internal standard. Only 1 or 2 μg of the DNA digests was loaded on the capillary column and analyzed according to the method described earlier. In the HPG

Table 1. Summary of HNE-dG Adducts in AD and Controls[a]

	subject	brain region	gender (F/M)	age (years)	PMI (h)	Braak score	HNE-dG per 10^9
AD	J	HPG	F	65	3.0	6	410
	B	HPG	M	69	3.5	6	390
	A	HPG	M	72	2.8	6	554
	G	HPG	M	76	3.0	N/A	287
	D	HPG	F	79	2.0	6	351
	F	HPG	F	79	3.0	6	1018
	I	HPG	F	90	4.5	6	185
	E	HPG	M	93	3.0	6	1256
		$n = 8$	**4M/4F**	**77.9 ± 9.7**	**3.1 ± 0.7**	**6.0 ± 0.0**	**556 ± 379**
control	L	HPG	F	65	3.0	0	170
	K	HPG	M	72	3.0	0.5	732
	M	HPG	M	80	3.5	1	814
	H	HPG	F	92	2.3	2	122
	C	HPG	M	105	3.0	3	486
		$n = 5$	**3M/2F**	**82.8 ± 16.0**	**3.0 ± 0.4**	**1.3 ± 1.2**	**464 ± 316**
P value				**0.699**	**0.379**		**0.452**
AD	T	IPL	F	65	3.0	6	220
	R	IPL	F	79	2.0	6	187
	S	IPL	M	90	3.0	6	345
	U	IPL	M	93	3.0	6	202
		$n = 4$	**2M/2F**	**81.8 ± 12.7**	**2.8 ± 0.5**	**6.0 ± 0.0**	**238 ± 72**
control	P	IPL	F	65	3.0	0	500
	Q	IPL	M	80	3.5	1	1274
	V	IPL	M	80	3.5	1	54
	O	IPL	F	92	2.3	2	355
		$n = 4$	**2M/2F**	**79.3 ± 11.1**	**3.1 ± 0.6**	**1.0 ± 0.8**	**545 ± 520**
P value				**0.776**	**0.423**		**0.286**

[a] Values are expressed as means ± SEM. PMI refers to postmortem interval. The *P* value was calculated from unpaired Student's *t*-test.

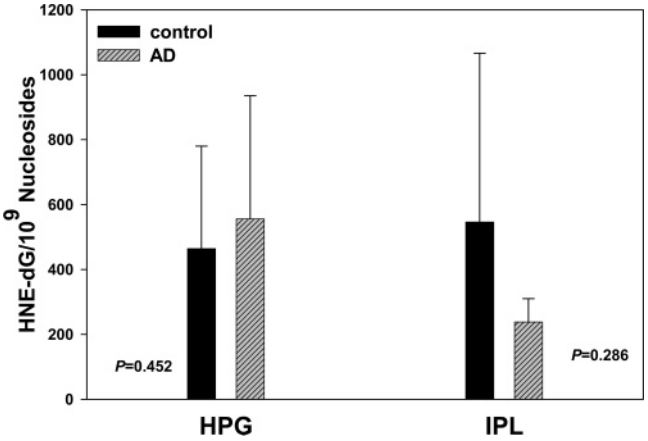

Figure 5. Distribution of HNE-dG adducts in the HPG region and IPL regions of AD and control subjects.

region of AD subjects, the level of the HNE-dG adducts (per 10^9 normal nucleosides) ranged from 185 to 1256, with an average value of 556 ± 379 (Table 1). In control subjects, the levels of HNE-dG adducts (per 10^9 normal nucleosides) ranged from 122 to 814, where the average value was 464 ± 316 (Figure 5). No statistically significant difference between AD subjects and controls was observed from the HPG region ($P = 0.452$). In the IPL region of AD subjects, the level of the HNE-dG adducts (per 10^9 normal nucleosides) ranged from 187 to 345, and the average value was 238 ± 72. In contrast, levels of HNE-dG adducts in control subjects (per 10^9 normal nucleosides) ranged from 54 to 1274, and the average value was 546 ± 520 (Figure 5). No statistically significant difference between AD subjects and controls in the IPL region was found either ($P = 0.286$). Results from this capLC-nanoESI-IDMS/MS method were consistent with ^{32}P-postlabeling method values of 400−600 adducts per 10^9 normal adducts in hippocampus using 10 μg of DNA. Our results support the conclusion of Eder et al. that the HNE-dG adduct levels are not altered in the AD subjects relative to controls (*35*). Using short postmortem interval autopsy brain specimens, our study indicated that no substantial difference in HNE-dG adduct level was detected between AD and age-matched control subjects even though previous studies showed increased free HNE concentrations in the brain tissue of AD subjects. A steady state level of endogenous HNE-mediated DNA damage appears to exist in both AD and control brain tissue as a result of insult from lipid peroxidation products. HNE-dG adduct levels do not appear to be a useful marker for the occurrence or the extent of oxidative stress in AD. The relatively low levels of HNE-dG adducts in brain tissue may reflect their intrinsic low tissue abundance, high reactivity with cytoplasmic proteins, or efficient repair of HNE-dG adducts. There is evidence to suggest that HNE-dG adducts are repaired by the nucleotide excision repair (NER) pathway in a dose- and time-dependent manner; the repair kinetics demonstrates that the excision rate is faster than the rate of gap filling/DNA synthesis (*36*). The relatively efficient *in vivo* removal of all four isomers of HNE-dG adducts may partially explain their lack of accumulation in AD as compared to controls. In addition, HNE has been shown to be capable of diffusing to different subcellular compartments and interacting with many different cellular proteins, including glutathione (*37*), tau (*38*, *39*), and histones (*40*). At present, no quantitative information is available on the relative abundance of HNE-protein conjugates as compared to HNE-dG adducts.

In summary, a capLC-nanoESI-IDMS/MS method was developed for selective identification and quantification of deoxyguanosine adducts of HNE. The separation of HNE-dG adducts from intact nucleosides in the enzymatic hydrolysates of DNA was achieved using capillary HPLC columns. The sensitivity of this method was determined to be approximately 24 amol (10 fg) of HNE-dG on capillary LC column. The developed method was applied to quantification of HNE-dG adducts in brain tissues from AD and control samples. Only 1−2 μg of DNA was used, and HNE-dG adduct levels in AD samples were observed at 556 ± 379 and 238 ± 72 adducts per 10^9 normal nucleosides in HPG and IPL regions, respectively. The described

method provides an alternative to the conventional ^{32}P-postlabeling method in detecting HNE-dG adducts with comparable sensitivity but without the use of radioisotopes.

Acknowledgment. We thank the University of Kentucky Mass Spectrometry Facility (www.rgs.uky.edu/ukmsf) and Sanders-Brown Center on Aging for the valuable resources and Dr. Jack Goodman for helpful discussions. The support for this work was from NIH (5P50-AG05114 and 5P01-AG05119) and the Abercrombie Foundation. X.L. acknowledges support from the Research Challenge Trust Funds Fellowship from the University of Kentucky.

References

(1) Uchida, K. (2003) 4-Hydroxy-2-nonenal: A product and mediator of oxidative stress. *Prog. Lipid Res. 42*, 318−343.

(2) Spiteller, G. (1998) Linoleic acid peroxidation—the dominant lipid peroxidation process in low-density lipoprotein—and its relationship to chronic diseases. *Chem. Phys. Lipids 95*, 105−162.

(3) Benedetti, A., Comporti, M., and Esterbauer, H. (1980) Identification of 4-hydroxynonenal as a cytotoxic product originating from the peroxidation of liver microsomal lipids. *Biochim. Biophys. Acta 620*, 281−296.

(4) Esterbauer, H., Benedetti, A., Lang, J., Fulceri, R., Fauler, G., Comporti, M., and Ferrali, M. (1986) Studies on the mechanism of formation of 4-hydroxynonenal during microsomal lipid peroxidation. Evidence for aldehydes bound to liver microsomal protein following CCl4 or BrCCl3 poisoning. *Biochim. Biophys. Acta 876*, 154−166.

(5) Esterbauer, H., Schaur, R. J., and Zollner, H. (1991) Chemistry and biochemistry of 4-hydroxynonenal, malonaldehyde and related aldehydes. *Free Radical Biol. Med. 11*, 81−128.

(6) Kaneko, K., Yoshida, K., Arima, K., Ohara, S., Miyajima, H., Kato, T., Ohta, M., and Ikeda, S. I. (2002) Astrocytic deformity and globular structures are characteristic of the brains of patients with aceruloplasminemia. *J. Neuropathol. Exp. Neurol. 61*, 1069−1077.

(7) Weigel, A. L., Handa, J. T., and Hjelmeland, L. M. (2002) Microarray analysis of H_2O_2-, HNE-, or tBH-treated ARPE-19 cells. *Free Radical Biol. Med. 33*, 1419−1432.

(8) Chung, F.-L., Pan, J., Choudhury, S., Roy, R., Hu, W., and Tang, M.-S. (2003) Formation of *trans*-4-hydroxy-2-nonenal- and other enal-derived cyclic DNA adducts from ω-3 and ω-6 polyunsaturated fatty acids and their roles in DNA repair and human p53 gene mutation. *Mutat. Res. 531*, 25−36.

(9) Chung, F. L., Young, R., and Hecht, S. S. (1984) Formation of cyclic 1,N^2-propanodeoxyguanosine adducts in DNA upon reaction with acrolein or crotonaldehyde. *Cancer Res. 44*, 990−995.

(10) Eder, E., Hoffman, C., Bastian, H., Deininger, C., and Scheckenbach, S. (1990) Molecular mechanisms of DNA damage initiated by alpha, beta-unsaturated carbonyl compounds as criteria for genotoxicity and mutagenicity. *Environ. Health Perspect. 88*, 99−106.

(11) Winter, C. K., Segall, H. J., and Haddon, W. F. (1986) Formation of cyclic adducts of deoxyguanosine with the aldehydes *trans*-4-hydroxy-2-hexenal and *trans*-4-hydroxy-2-nonenal in vitro. *Cancer Res. 46*, 5682−5686.

(12) Zarkovic, K. (2003) 4-Hydroxynonenal and neurodegenerative diseases. *Mol. Aspects Med. 24*, 293−303.

(13) Markesbery, W. R., Kryscio, R. J., Lovell, M. A., and Morrow, J. D. (2005) Lipid peroxidation is an early event in the brain in amnestic mild cognitive impairment. *Ann. Neurol. 58*, 730−735.

(14) Williams, T. I., Lynn, B. C., Markesbery, W. R., and Lovell, M. A. (2005) Increased levels of 4-hydroxynonenal and acrolein, neurotoxic markers of lipid peroxidation, in the brain in Mild Cognitive Impairment and early Alzheimer's disease. *Neurobiol. Aging*, in press.

(15) Sharma, R. A., and Farmer, P. B. (2004) Biological relevance of adduct detection to the chemoprevention of cancer. *Clin. Cancer Res. 10*, 4901−4912.

(16) Singh, R., and Farmer, P. B. (2006) Liquid chromatography-electrospray ionization-mass spectrometry: The future of DNA adduct detection. *Carcinogenesis 27*, 178−196.

(17) Yi, P., Zhan, D., Samokyszyn, V. M., Doerge, D. R., and Fu, P. P. (1997) Synthesis and ^{32}P-postlabeling/high-performance liquid chromatography separation of diastereomeric 1,N^2-(1,3-propano)-2′-deoxyguanosine 3′-phosphate adducts formed from 4-hydroxy-2-nonenal. *Chem. Res. Toxicol. 10*, 1259−1265.

(18) Chung, F. L., Nath, R. G., Ocando, J., Nishikawa, A., and Zhang, L. (2000) Deoxyguanosine adducts of t-4-hydroxy-2-nonenal are endogenous DNA lesions in rodents and humans: Detection and potential sources. *Cancer Res. 60*, 1507−1511.

(19) Chung, F. L., and Zhang, L. (2002) Deoxyguanosine adducts of tert-4-hydroxy-2-nonenal as markers of endogenous DNA lesions. *Methods Enzymol. 353*, 523−536.

(20) Wacker, M., Schuler, D., Wanek, P., and Eder, E. (2000) Development of a 32P-postlabeling method for the detection of 1,N^2-propanodeoxyguanosine adducts of *trans*-4-hydroxy-2-nonenal in vivo. *Chem. Res. Toxicol. 13*, 1165−1173.

(21) Chandra, A., and Srivastava, S. K. (1997) A synthesis of 4-hydroxy-2-trans-nonenal and 4-(^{3}H) 4-hydroxy-2-trans-nonenal. *Lipids 32*, 779−782.

(22) Rees, M. S., van Kuijk, F. J. G. M., Siakotos, A. N., and Mundy, B. P. (1995) Improved synthesis of various isotope labeled 4-hydroxyalkenals and peroxidation intermediates. *Synth. Commun. 25*, 3225−3236.

(23) Wenner, B. R., Lovell, M. A., and Lynn, B. C. (2004) Proteomic analysis of human ventricular cerebrospinal fluid from neurologically normal, elderly subjects using two-dimensional LC-MS/MS. Factors that affect ion trap data-dependent MS/MS in proteomics. *J. Proteome Res. 3*, 97−103.

(24) Liu, X., Lovell, M. A., and Lynn, B. C. (2005) Development of a method for quantification of acrolein-deoxyguanosine adducts in DNA using isotope dilution-capillary LC/MS/MS and its application to human brain tissue. *Anal. Chem. 77*, 5982−5989.

(25) National Institute on Aging and the Reagan Institute Working on Group Diagnostic Criteria for the Neuropathological Assessment of Alzheimer's Disease (1997) Consensus recommendations for the postmortem diagnosis of Alzheimer's disease. *Neurobiol. Aging 18*, S1−S2.

(26) Braak, H., Braak, E., Yilmazer, D., de Vos, R. A., Jansen, E. N., and Bohl, J. (1996) Pattern of brain destruction in Parkinson's and Alzheimer's diseases. *J. Neural Transm. 103*, 455−490.

(27) Lovell, M. A., Xie, C., and Markesbery, W. R. (2001) Acrolein is increased in Alzheimer's disease brain and is toxic to primary hippocampal cultures. *Neurobiol. Aging 22*, 187−194.

(28) Wang, H., Kozekov, I. D., Harris, T. M., and Rizzo, C. J. (2003) Site-specific synthesis and reactivity of oligonucleotides containing stereochemically defined 1,N^2-deoxyguanosine adducts of the lipid peroxidation product *trans*-4-hydroxynonenal. *J. Am. Chem. Soc. 125*, 5687−5700.

(29) Wacker, M., Wanek, P., and Eder, E. (2001) Detection of 1,N^2-propanodeoxyguanosine adducts of *trans*-4-hydroxy-2-nonenal after gavage of *trans*-4-hydroxy-2-nonenal or induction of lipid peroxidation with carbon tetrachloride in F344 rats. *Chem.-Biol. Interact. 137*, 269−283.

(30) Fernandes, P. H., Wang, H., Rizzo, C. J., and Lloyd, R. S. (2003) Site-specific mutagenicity of stereochemically defined 1,N^2-deoxyguanosine adducts of *trans*-4-hydroxynonenal in mammalian cells. *Environ. Mol. Mutagen. 42*, 68−74.

(31) Novotny, M. (1985) Analytical characteristics of packed capillary columns. *J. Chromatogr. Libr. 30*, 19−34.

(32) Davidson, J. N. (1972) *The Biochemistry of Nucleic Acids*, Chapman and Hall, New York.

(33) Markesbery, W. R., and Lovell, M. A. (1998) Four-hydroxynonenal, a product of lipid peroxidation, is increased in the brain in Alzheimer's disease. *Neurobiol. Aging 19*, 33−36.

(34) Lovell, M. A., Ehmann, W. D., Mattson, M. P., and Markesbery, W. R. (1997) Elevated 4-hydroxynonenal in ventricular fluid in Alzheimer's disease. *Neurobiol. Aging 18*, 457−461.

(35) Gotz, M. E., Wacker, M., Luckhaus, C., Wanek, P., Tatschner, T., Jellinger, K., Leblhuber, F., Ransmayr, G., Riederer, P., and Eder, E. (2002) Unaltered brain levels of 1,N^2-propanodeoxyguanosine adducts of *trans*-4-hydroxy-2-nonenal in Alzheimer's disease. *Neurosci. Lett. 324*, 49−52.

(36) Choudhury, S., Pan, J., Amin, S., Chung, F. L., and Roy, R. (2004) Repair kinetics of *trans*-4-hydroxynonenal-induced cyclic 1,N^2-propanodeoxyguanine DNA adducts by human cell nuclear extracts. *Biochemistry 43* (23), 7514−7521.

(37) Sultana, R., and Butterfield, D. A. (2004) Oxidatively modified GST and MRP1 in Alzheimer's disease brain: Implications for accumulation of reactive lipid peroxidation products. *Neurochem. Res. 29*, 2215−2220.

(38) Liu, Q., Smith, M. A., Avila, J., DeBernardis, J., Kansal, M., Takeda, A., Zhu, X., Nunomura, A., Honda, K., and Moreira, P. I. (2005) Alzheimer-specific epitopes of tau represent lipid peroxidation-induced conformations. *Free Radical Biol. Med. 38*, 746−754.

(39) Mattson, M. P., Fu, W., Waeg, G., and Uchida, K. (1997) 4-Hydroxynonenal, a product of lipid peroxidation, inhibits dephosphorylation of the microtubule-associated protein tau. *NeuroReport 8*, 2275−2281.

(40) Drake, J., Petroze, R., Castegna, A., Ding, Q., Keller, J. N., Markesbery, W. R., Lovell, M. A., and Butterfield, D. A. (2004) 4-Hydroxynonenal oxidatively modifies histones: Implications for Alzheimer's disease. *Neurosci. Lett. 356*, 155−158.

TX0502903